Short thesis for the degree of doctor of philosophy (PhD)

Chemical characterization of Gd(III) and Mn(II) complexes formed with chelating ligands containing malonate pendants

by Abraham Estifanos Debretsion

Supervisor: Dr. Ferenc K. Kálmán

UNIVERSITY OF DEBRECEN
Doctoral School of Chemistry

Debrecen, 2025

I. Introduction and objectives

Over the past forty years, magnetic resonance imaging (MRI) has emerged as a highly effective diagnostic technique for soft tissues of human anatomy, physiology, and pathophysiology. MRI is a medical imaging technique with high spatial resolution and no ionizing radiation. MRI uses the principle of nuclear magnetic resonance (NMR), thus radio frequency generates diagnostic images thanks to the interaction of that with water protons. Since, circa 60% of our body is water, MRI can provide images of various tissue types by measuring the T_1 (longitudinal) and T_2 (transverse) relaxation rates of protons due to the different water content in the healthy and diseased tissues. The relaxation rate of the protons can be enhanced by means of the so-called MRI contrast agents (CAs) administered intravenously to the patients, thus improving the quality of the MRI images.

In the U.S., the demand for gadolinium-based contrast agents has grown to approximately 30% to 45% of all clinical MRI diagnoses every year. Most of the MRI contrast agents in the market are gadolinium-based contrast agents (GBCAs), even though manganese-based one also existed.

The general criteria for metal chelates to be MRI contrast agents are high relaxivity (relaxation enhancement effect of the complex in solution regarding to 1 mM concentration), high thermodynamic stability, high inertness, good solubility, low osmolality and so on. Obviously, high relaxivity is a key parameter, since with higher relaxivity, less complex needs to be administered to achieve the same contrast enhancement. Furthermore, the suitable thermodynamic stability and high inertness collectively determine the lower toxicity of the CAs by preventing the *in vivo* dissociation of the applied chelates, the liberation of the paramagnetic metal ion. The free Gd^{3+} ion is toxic, its LD_{50} value is around 0.1-0.3 mmol/kg, so that has to be enclosed by ligands.

In order to prevent the liberation of the Gd^{3+} in the body, that is complexed with polyamino-polycarboxylate chelators bearing high stability and inertness. Upon the release of the Gd^{3+}, it can interact with the small bioligands (carbonate, phosphate, amino acids, etc.), proteins, enzymes and interfere with biological processes (signaling paths).

Initially, the risk of GBCAs was considered negligible, but in 2006, the illness known as nephrogenic systemic fibrosis (NSF) was recognized as a debilitating and fatal disease and linked to the *in vivo* dissociation of Gd^{3+} chelates. In September 2010, the US Food and Drug Administration (FDA) ordered screening for those who have acute kidney harm or severe renal disease. Finally, they classified the clinically approved GBCAs as Group I agents for linear (gadodiamide, gadopentetate dimeglumine, gadoversetamide) and Group II agents for macrocyclic (gadobenate dimeglumine, gadobutrol, gadoteric acid, gadoteridol). Later, the FDA and the European Medicines Agency (EMA) decided to partially suspend the linear GBCAs gadodiamide, gadopentetic acid, and gadoversetamide.

The discovery of NSF induced a still growing research to replace the compromised agents with safer alternatives. A solution to this problem is to prevent the decomplexation of GBCAs by increasing their inertness through developing more rigid chelates. On the other hand, the desired goal of reducing the risk of serious intoxication can be achieved by applying essential paramagnetic metal ions, such as Mn(II) or Fe(III), to develop biocompatible CAs.

The kinetic inertness has become of critical importance compared to thermodynamic stability for MRI contrast agents intended for practical use. The increase in the inertness of the complexes can be achieved by increasing the rigidity of the macrocyclic ring, for example, by incorporating the donor atoms into rigid structures (amine $\rightarrow$ pyridine), or in order to avoid the fast dechelation, the highly basic donor atoms can be replaced with less basic ones (amine $\rightarrow$

etheric oxygen). However, these modifications also come with disadvantages, as they cause the loss of the substitutability of the given atom(s), resulting in a drop in the denticity of the ligand. Nevertheless, the proper denticity can be achieved by incorporating side chain(s) which contains more than one donors. Based on previous results, we knew that the O-pyclen macrocycle has a rigid structure, so it seemed to be a good platform for designing ligands suitable for the coordination of both Gd(III) and Mn(II) ions using malonate pendants. Furthermore, since the coordination number of the Mn(II) ion is lower (its complexes typically exhibit a coordination number (CN) of 7) than that of the Gd(III) (CN = 9), the H_2OPMMA with its 6 donor atoms appeared to be suitable for Mn(II) complexation, while the H_2OPDMA (8 donors) for the chelation of Gd(III). Thus, in both cases, there is also possibility for a water molecule to be coordinated in the inner sphere of the complexes.

For these reasons, the objectives of this research were:

(i) To synthesize O-pyclen-based macrocyclic ligands (Figure 1) bearing malonate pendant arms for Gd^{3+} and Mn^{2+} complexation as potential MRI agents.

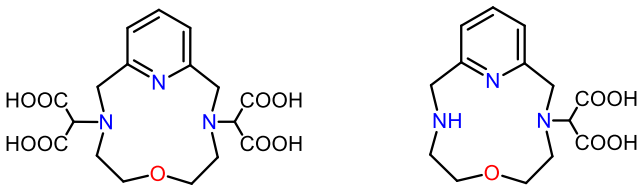

H_4OPDMA **H_2OPMMA**

Figure 1. Structure of the investigated ligands.

(ii) To characterize the relaxation properties of the complexes to understand the relations between the structure of the chelates and the parameters influencing their relaxivities.

(iii) To investigate the thermodynamic stability and inertness of the complexes, the two factors, which are essential for the safe *in vivo* applications.

II. Experimental methods

The commercial reagents/solvents purchased from Sigma-Aldrich (St. Louis, MO, USA) and Fluorochem Ltd. (Hadfield, United Kingdom) were used without further purification. The metal salts and other materials used in the studies were purchased from commercial sources and used without further purification (the purity of the compounds was higher than metal salts is 99.0%). Standardized Na_2H_2EDTA was used to determine the concentration of the metal ion solutions using complexometric titrations in the presence of different indicators (Ln^{3+} - xylenol orange, Cu^{2+} - murexide). The complexes were prepared by mixing known concentrated solutions of the components in 1:1 stoichiometric ratio, followed by pH adjustment. Deionized Milli-Q water was used for the preparation of all aqueous solutions (equilibrium/kinetic/relaxometric studies).

II.1. HPLC measurement

A Waters Alliance 2690 HPLC unit equipped with Waters 996 PDA detector, and a Phenomenex Luna C18(2) 100Å 150 x 4.6 mm 5 micron column were used to follow the synthetic reactions. This system was also used to confirm the formation of the complexes and to investigate the stability of the solutions. The separation and purification of the ligands were carried out with a YL9100 HPLC system (Korea) equipped YL9101S degasser, YL9110S pump, YL9120S UV/VIS detector, Phenomenex Luna Prep C18(2) 100Å 250 × 21.2 mm 5 micron 00G-4252-P0-AX column and Sigma-Aldrich CHROMASOLV® Plus solvents.

II.2. Mass spectrometry measurement

Mass spectra were recorded in the Laboratory of Instrumental Analysis, Department of Inorganic and Analytical Chemistry, University of Debrecen by using a maXis II UHR ESI-QTOF MS Bruker instrument. The purity of the final

products were higher than 98.0% determined by reverse-phase HPLC with UV−Vis detection at 220 and 260 nm.

II.3. pH potentiometric studies

Protonation constant of the ligands (H_4OPDMA and H_2OPMMA) and the protonation and stability constants of their metal ion complex were determined using pH-potentiometric titrations supported by relaxometric measurements in the case of the $[Gd(OPDMA)]^-$. The analytical concentration of the ligand stock solutions was calculated from the ligand titrations. A Metrohm 888 Titrando workstation equipped with a Metrohm-6.0233.100 combined electrode were used for the pH-potentiometric titrations. KH-phthalate (pH=4.005) and borax (pH=9.177) buffers were applied for the electrode calibration. The samples were kept under N_2 atmosphere during the titrations to avoid the effect of CO_2. The 6.0 mL samples were at 25 °C and stirred. 0.15 M NaCl was used to keep the ionic strength constant. The titrations were performed by using 0.2 M NaOH (dwell time = 40 s). The concentration of the ligands and the metal ions were in the range of 1.5 - 2.0 mM in 1 to 1 ratio. 130-200 volume–pH data pairs were recorded in the titrations in the pH range of 1.7-12.0. The Irving factor of the electrode and the K_w were evaluated from acid-base titration in which 0.01 M HCl was used. PSEQUAD program was used to gain the equilibrium constants. Since the formation of the $[Gd(OPDMA)]^-$ occurs under pH 2, 11 out-of-cell samples were prepared in the acid concentration range 0.001-0.08 M (I=$[Na^+]$+$[H^+]$=0.15 M) and their T_1 and T_2 relaxation times were measured after equilibration time (2 hours). In order to avoid the misleading information may be originated from the slow complex formation in acidic condition, the pre-prepared $[Gd(OPDMA)]^-$ complex was mixed with HCl solution. To determine the relaxation times, Bruker Minispec MQ-60 NMR Analyzer was used (more details below).

II.4. UV-Vis spectrophotometry

The rate of the transmetallation occurs between the $[Gd(OPDMA)]^-$ complex and Cu(II) ions was studied at 37 °C in the presence of 0.15 M NaCl by monitoring the absorbance change at 260 nm using a Cary 100 Bio UV-vis spectrophotometer (pH range 2.0 – 4.0). The concentration of the complex was 0.1 mM, while that of the Cu(II) ion was 10-, 20- and 40-times higher to ensure pseudo-first order conditions. The pH was maintained by means of chloroacetic acid (pK_a=2.9) and 1,4-dimethylpiperazine (pK_a=4.2) buffers in 50 mM concentration.

Based on preliminary experiments, the dissociation rate of the [Mn(OPMMA)] was found to be fast for conventional spectrophotometry, therefore stopped-flow technique was used to investigate the reaction occurs between the complex and the Cu(II) ion. The concentration of the complex and the Cu(II) 0.1 and 2.0 mM, respectively. The reactions were carried out at 25 °C, in the presence of 0.15 M NaCl by an Applied Photophysics DX-17MV stopped-flow machine. The decomplexation was followed at 280 nm in the pH range 3.9-5.0. For pH stabilization, N-methylpiperazine (NMP, log K_2^H = 4.90) was used in 20 mM concentration, as a buffer.

The Micromath Scientist computer program (version 2.0, Salt Lake City, UT, USA) was used to fit the time-absorbance data pairs and the pseudo-first-order rate constants (k_{obs}) by using a standard least-squares procedure.

II.5. ^{1}H-relaxometry

The dissociation reaction of the $[Gd(OPDMA)]^-$ (1.0 mM) in the presence of Eu(III) ion (20 mM) at 37 °C and 0.15 M NaCl ionic strength was studied by measuring the $1/T_2$ relaxation rates of the samples on a Bruker Minispec MQ-60 NMR Analyzer (pH range 2.0 – 4.0). The $1/T_2$ values of the samples were determined with the Carl–Purcell–Meiboom–Gill (CPMG) spin-echo pulse sequence. The pH was maintained by means of chloroacetic acid (pK_a=2.9) and

1,4-dimethylpiperazine (pK_a=4.2) buffers in 50 mM concentration. The experimental data were analyzed by the Scientist program calculating the k_{obs} values.

The ^{1}H longitudinal (T_1) for [Gd(OPDMA)]$^-$ and [Mn(OPMMA)] as well as the transverse (T_2) relaxation times for [Mn(OPMMA)] complex were determined by using Bruker Minispec MQ-20 and MQ-60 NMR analyzers. The temperature was set to 25.0 or 37.0 (±0.2) °C, and maintained with a circulating water bath thermostat. For T_1 determination, inversion recovery method (180°–τ–90°; 6–8 data points at 10 different τ delay times) was used, while the T_2 relaxation times were determined by the aforementioned CPMG method in the presence of HEPES buffer (50 mM, pH = 7.4) and 0.15 M NaCl.

II.6. NMR measurements

The NMR spectra were recorded on Bruker Avance II 500 MHz spectrometer (Bruker, Billerica, MA, USA) using deuterated solvents (chemical shifts are given as δ values with reference to the deuterated solvents (D_2O, CD_3CN) and the coupling constants are reported in Hz).

II.7. ^{1}H NMRD and ^{17}O NMR studies

In order to determine the parameters govern the relaxivity of the paramagnetic metal complexes ^{1}H NMRD and ^{17}O NMR measurements were carried out.

^{1}H NMRD measurements were performed on samples containing the [Gd(OPDMA)]$^-$ (pH = 7.4) and [Mn(OPMMA)] (pH = 8.0) in 1.0 mM concentration (in the case of [Mn(OPMMA)] 10% ligand excess was applied) at 25.0 and 37.0 °C, on a Stelar SMARTracer Fast Field Cycling relaxometer (0.01−10 MHz) and a Stelar high field relaxometer (10-128 MHz). The temperature was maintained by a VTC91 temperature control unit and gas flow, and it was calibrated by a Pt resistance probe.

In the ^{17}O NMR experiments, the transverse ($1/T_2$) relaxation rates and chemical shifts of an aqueous solution of the complexes (the concentration and the pH were set to 21.4 mM and 7.0 for the $[Gd(OPDMA)]^-$ as well as 6.4 mM and 8.0 for the [Mn(OPMMA)], respectively) and of a diamagnetic reference ($HClO_4$ acidified water, pH = 3.3) were measured in the temperature range 273–348 K using a Bruker Avance 400 (9.4 T, 54.2 MHz) spectrometer. The temperature was determined according to the method proposed by Raiford. The $1/T_2$ values were determined by CPMG technique. In order to avoid the susceptibility corrections to the chemical shifts, a glass sphere in an 10 mm NMR tube was applied. ^{17}O enriched water (10% $H_2{}^{17}O$, CortecNet) was added to the solutions to reach around 1% enrichment. The least-squares fit of the ^{17}O NMR and NMRD data was performed by means of Visualiseur/Optimiseur running on a MATLAB 8.3.0 (R2014a) platform.

II.8. Determination of *q* for $[Gd(OPDMA)]^-$

In order to determine the number of the water molecules in the inner sphere of the $[Gd(OPDMA)]^-$ luminescence lifetimes of the $[Eu(OPDMA)]^-$ complex were measured on an Agilent Cary Eclipse Fluorescence spectrophotometer. The decay of the emission intensity at 614 nm followed by an excitation at 268 nm was recorded. Measurements were performed in both H_2O and D_2O solutions. The settings were as follows: gate time: 0.1 ms (1.0 ms in D_2O); delay time: 0.1 ms; flash count: 1; total decay time: 5.0 ms (15 ms in D_2O); 10 cycles; PMT detector: 650 mV. At least three decay curves were collected for each sample, and all lifetimes were analyzed as monoexponential decay. The reported lifetimes are an average of at least three measurements. The number of *q*, 1.2/1.3 was found to be the same at pH = 3 and pH = 7.

IV.9. DFT calculations

The ground state geometry of the $[Gd(OPDMA)]^{-}$ was computed using the Gaussian 09 software package (ES64L-G09 RevE.01) at the DFT level of theory. In this calculation, the TPSSh exchange-correlation functional in combination with Grimme's DFT-D3 approach including BJ-damping was used together with the quasi-relativistic effective core potential including 53 electrons in the core (ECP53MWB) with the corresponding (7s6p5d)/[5s4p3d] basis sets for Gd. All other atoms were treated with the 6-311G(d,p) basis set. The effect of the solvent was taken into account by using the polarizable continuum model (PCM). Single-point frequency calculations at the same level of theory were also carried out for the ground state geometry.

Geometry optimization of the [Mn(OPMMA)] complex was computed by using Gaussian 09 (EM64L-G09RevC.01) at DFT level of theory using the hybrid-meta-GGA TPSSh functional combined with the aug-cc-pVTZ-J for Mn(II) which is described by a (25s17p10d3f2g)/[17s10p7d3f2g] contraction scheme. The *def2*-TZVP basis set was used for non-metal atoms (H, C, N and O). All calculations accounted for solvent effect using the continuum model (PCM) for water. Single-point frequency calculations were carried out with the same functional and basis sets for the ground state geometries which represented true minima on the potential energy surface.

Single-point calculation for the optimized geometry was carried out to predict the ^{17}O hyperfine coupling constant. This calculation was computed through the ORCA package using the TPSSh functional. In this calculation, the aug-cc-pVTZ-J basis set was used for Mn(II) and the other atoms were treated by the EPR-III basis sets of Barone which triple-ζ basis set includes diffuse functions, double d-polarizations and a single set of f-polarization functions. The resolution of identity and chain of spheres exchange (RIJCOSX) approximation was used to accelerate the calculations and tight SCF convergence criteria were employed.

III. New scientific results

We have studied in detail the physicochemical characteristics of $[Gd(OPDMA)]^-$ and [Mn(OPMMA)] complexes. This includes the thermodynamic stability, kinetic inertness and relaxation properties. Additionally, in order to get a better insight the solution structure of the complexes studied, DFT calculations were also performed.

III.1. Equilibrium study of H_4OPDMA and its Gd^{3+} complex

Five protonation constants were found for the $OPDMA^{4-}$ ligand, which are listed in Table 1. Since the basicity of the donor atoms located at the ligand backbone has the highest influence on the formation of the so-called "in-cage" complex, the sum of those ($\Sigma\log K_2^H$) has been calculated and compared with the corresponding values gained for H_4DTPA, H_4AAZTA, H_3PCTA and H_4DOTA.

Table 1. Protonation constants ($\log K_i$) of $OPDMA^{4-}$ and the comparative ligands, protonation and stability constants of their Gd^{3+} complexes
(T = 25 °C, 3σ standard deviations are indicated in parenthesis).

	$OPDMA^{4-}$	**$DTPA^{5-}$**	**$AAZTA^{4-}$**	**$PCTA^{3-}$**	**$DOTA^{4-}$**
$\log K_1$	7.14(5)	9.93	11.23	11.36	11.08
$\log K_2$	6.99(2)	8.37	6.52	7.35	9.23
$\log K_3$	3.17(4)	4.18	3.78	3.83	4.24
$\log K_4$	2.23(4)	2.71	2.24	2.12	4.18
$\log K_5$	2.02(5)	2.00	1.56	1.29	1.88
$\Sigma\log K_2^H$ [a]	**14.13**	**18.30**	**17.75**	**18.71**	**20.31**
$\log K_{GdL}$	18.01(7)	22.03	20.24	20.39	24.7[f]
$\log K_{GdL}^H$	2.09(5)	1.96	1.89	–	–
pGd[b]	**14.8**	**15.5**	**13.4**	**13.1**	**16.2**

[a] $\log K_1 + \log K_2$; [b] pH=7.4; $c_L = c_M = 0.01$ mmol/dm^3

The results show that the basicity of H_4OPDMA is orders of magnitude lower than that of the ligands used for comparative purposes.

The stability constant of the $[Gd(OPDMA)]^-$ is at least two orders of magnitude lower than those of the other complexes compared (Table 1). The pGd of $[Gd(OPDMA)]^-$ is also lower than that of $DTPA^{5-}$ and $DOTA^{4-}$ complexes, but higher than that of the $AAZTA^{4-}$ and $PCTA^{3-}$ chelates (Table 1).

A protonation constant was also found for $[Gd(OPDMA)]^-$, which shows slightly higher value than that was found for DTPA and AAZTA complexes. According to the DFT calculations (*see below*), one carboxylate group is not involved in the coordination, thus the protonation of this carboxylate is easier at acidic pH.

III.2. Inertness of $[Gd(OPDMA)]^-$

The metal exchange reactions of $[Gd(OPDMA)]^-$ was studied at 37 °C, where Cu(II) and Eu(III) ions were applied in high excess to ensure pseudo-first order conditions.

During the fitting procedure, we found that the role of the spontaneous and metal-assisted dissociation pathways is negligible.

The obtained rate constant and the calculated dissociation half-life ($t_{1/2}$) are given in Table 2, together with the corresponding data for the Gd^{3+} complexes of $DTPA^{5-}$, $AAZTA^{4-}$, $PCTA^{3-}$ and $DOTA^{4-}$.

Comparing the $t_{1/2}$ values calculated for 25 °C, one can conclude that, the inertness of $[Gd(OPDMA)]^-$ is higher than that of the open-chain DTPA and AAZTA, but 3-4 orders of magnitude lower than that obtained for the macrocyclic PCTA and DOTA chelates. Interestingly, there is a slight (~30%) difference in the k_1 value depending on whether the exchange reactions were performed with Eu^{3+} or Cu^{2+} ions. However, we could not prove the presence of the metal-assisted pathway, the possible formation of dinuclear complexes with the exchanging metal ions may occur, which is more likely with Cu(II). The formation of the

dinuclear complexes can open up the structure of the coordination cavity which can accelerate the proton-assisted dechelation.

Table 2. Rate constants for the dissociation reactions of $OPDMA^{4-}$, $DTPA^{5-}$, $AAZTA^{4-}$, $PCTA^{3-}$ and $DOTA^{4-}$ complexes formed with Gd(III) ion and their half-lives calculated for pH 7.4 (25 °C / 37 °C, I =0.15 M (NaCl), charges are omitted for simplicity)

	OPDMA + Eu(III)	OPDMA + Cu(II)	DTPA	AAZTA	PCTA	DOTA
k_1 ($M^{-1}s^{-1}$)	~0.05 / 0.126(3)[a]	~0.07 / 0.175[a]	0.58	1.05	5.1×10^{-4}	8.4×10^{-6} / 2.0×10^{-5} [a]
$t_{1/2}$ (year)[b]	~11 / **4.4[a]**	~8 / **3.2[a]**	0.015	0.50	1.1×10^{3}	6.6×10^{4} / **2.7×10^{4} [a]**

[a] 37 °C; [b] $t_{1/2}=\ln2/k_{calc}$, pH=7.4

The dissociation half-life of our complex amounts to years at 37 °C if other dissociation pathways or enzymatic processes are not operative in the body, which is sufficient for *in vivo* applications.

III.3. Relaxation features of $[Gd(OPDMA)]^-$

The r_{1p} of CA candidates is a key parameter, which indicates their efficacy in relaxation enhancement. The r_{1p} values obtained for $[Gd(OPDMA)]^-$ at different field strengths (0.49 T and 1.41 T) and temperatures (25 and 37 °C) are compared to those of analogous chelates in Table 3.

There is no significant difference between the r_{1p} values of $[Gd(OPDMA)]^-$ and that of the q = 1 chelates, which indicates that one water molecule is coordinated in the inner sphere of the complex. The value of q was indeed determined by luminescence measurements on the Eu^{3+} complex delivering q = 1.2±0.1 value 25 °C.

The decrease of relaxivity values with increasing temperature (Table 3) indicates that the fast rotation of the complex limits the relaxivity, which behaviour is typical for low molecular weight Gd^{3+}-based chelates.

Table 3. r_{1p} values ($mM^{-1}s^{-1}$) determined for Gd(III) complexes of $OPDMA^{4-}$ and other ligands used for comparative purposes at pH=7.4, 25/37 °C and 20/60 MHz (charges are omitted for simplicity).

25/37 °C	OPDMA (q=1)	DTPA (q=1)	AAZTA (q=2)	PCTA (q=2)	DOTA (q=1)
0.47 T	4.5/3.7 4.5 (HSA)	4.7/3.8	7.1/5.2	6.9/5.2	4.7/3.5
1.4 T	4.3/3.4 4.4 (HSA)	4.2/3.4	6.7/4.8	6.3/4.8	4.3/3.1

Table 4. Best-fit parameters gained for $[Gd(OPDMA)]^{-}$ from the analysis of NMRD and ^{17}O NMR data along with the corresponding values found for the Gd^{3+} complexes formed with $DTPA^{5-}$, $AAZTA^{4-}$, $PCTA^{3-}$ and $DOTA^{4-}$ ligands (charges are omitted for simplicity).

Gd^{3+} chelates	OPDMA (q = 1)	DTPA (q = 1)	AAZTA (q = 2)	PCTA (q = 2)	DOTA (q = 1)
k_{ex}^{298} ($\times 10^6$ s^{-1})	73(12)	3.3	11.1	14	4.1
$\Delta H^{\ddagger}$ (kJ mol^{-1})	26.0(3)	52	20	45	50
$\Delta S^{\ddagger}$ (J mol^{-1} K^{-1})	-7(1)	+54	-43	+43	+47
$A/\hbar$ ($\times 10^6$ rad s^{-1})	-3.4(2)	-3.8	-3.8	-3.8	-3.7
τ_R^{298} (ps)	79(3)	58	74	70	77
E_r (kJ mol^{-1})	26(2)	17	20	–	16
τ_V^{298} (ps)	12(1)	25	30	15	11
Δ^2 ($\times 10^{20}$ s^{-2})	1.6(1)	0.46	0.26	0.59	0.16

The r_{1p} values determined in the presence of human serum albumin (c_{HSA} = 0.8 mM) indicate a negligible interaction between the complex and the protein (Table 3).

Based on the result gained from the simultaneous fitting of NMRD and ^{17}O NMR measurements (Table 4), one can conclude that the k_{ex}^{298} of $[Gd(OPDMA)]^-$ is the highest among all complexes compared. The negative value of $\Delta S^{\ddagger}$ indicates an associative mechanism for the water exchange process, in contrast with that of $[Gd(DTPA)]^{2-}$ and $[Gd(DOTA)]^-$ chelates, where a dissociative mechanism was found. The associative mechanism is a logical consequence of the 8-coordinated metal ion, according to the DFT calculations (see below). The lower activation enthalpy is also in accordance with this. The value of $A/\hbar$ (hyperfine coupling constant) is typical for Gd(III) complexes and in excellent agreement with that obtained by DFT calculations (-3.3×10^6 rad s^{-1}, *vide infra*). The rotational correlation time (τ_R) of our complex is close to those reported for other complexes of similar size. Interestingly, the electron spin relaxation of the $[Gd(OPDMA)]^-$ complex is relatively fast based on the higher Δ^2 (square zero field splitting energy) (Table 4). This phenomenon is likely the result of the less symmetric structure.

III.4. Calculated structure of $[Gd(OPDMA)]^-$

The structure of the $[Gd(OPDMA)]^-$ was calculated by DFT and optimized by considering an inner sphere water molecule and the presence of two second-sphere water molecules as well as the bulk solvent by using the polarized continuum model. The optimized structure of the $[Gd(OPDMA)]^-$ is shown in Figure 2.

The predicted structure shows a bicapped trigonal prismatic geometry where the ligand coordinates to the Gd^{3+} ion in a heptadentate manner. The inner sphere of the complex is completed with a H_2O molecule coordinated to the Gd^{3+} ion, yielding an overall coordination number of eight (CN=8). The Gd(III)-O_{water}

distance was found to be 2.47 Å which falls into the range of first coordination shell of water.

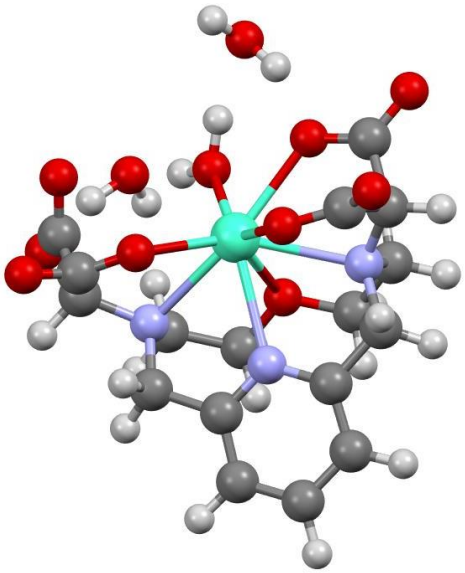

Figure 2. DFT calculated structure of $[Gd(OPDMA)]^{-}$ complex.

The ^{17}O hyperfine coupling constant was also calculated and estimated to be -3.33 $\times 10^6$ rad s^{-1} which is in perfect agreement with that obtained experimentally and verifies the structure in solution. Additionally, DFT also predicted a CN=9 coordination mode for the complex, where all carboxylate arms are bound to the Gd^{3+} ion completed with an inner-sphere H_2O molecule, however, the Gd(III)-O_{water} distance is calculated to be 2.61 Å which is relatively long, and the ^{17}O hyperfine coupling constant is unrealistic ($A/\hbar$ = -1.8×10^6 rad s^{-1}). Based on the results, one can conclude that the binding of the fourth carboxylate pendant is unfavorable, probably due to the electrostatic repulsion and/or steric reasons.

III.5. Equilibrium study of H_2OPMMA and its Mn^{2+} complex

The equilibrium calculations delivered four p*K*as for the $OPMMA^{2-}$ ligand which are presented in Table 5 and compared with the corresponding values obtained for $OPC2A^{2-}$ and 3,9-$PC2A^{2-}$ ligands.

The value of the logK_1 of $OPMMA^{2-}$ is three orders of magnitudes lower than that of 3,9-$PC2A^{2-}$, which is the result of the replacement of the trans-N to a less basic, etheric O donor. At the same time, the ”fusion” of the acetates into malonate increases the basicity, probably because of the presence of the unsubstituted amine and the presence of stronger H-bond between N and O donors.

Table 5. The protonation constants (logK_i) of the ligands ($OPMMA^{2-}$, $OPC2A^{2-}$ and 3,9-$PC2A^{2-}$) and the protonation and stability constants of their Mn^{2+} complexes.

	$OPMMA^{2-}$ [a]	$OPC2A^{2-}$	3,9-$PC2A^{2-}$
logK_1	9.17(5)	7.73	12.25
logK_2	8.19(5)	7.66	5.97
logK_3	3.26(7)	2.13	3.47
logK_4	1.29(9)	–	1.99
ΣlogK₂	***17.36***	***15.39***	***18.22***
logK_{MnL}	10.07(5)	13.03	17.09
logK_{MnHL}	–	2.40	2.14
log$K_{Mn(OH)L}$	11.00(7)	11.49	–
pMn[b]	***6.27***	***8.69***	***8.64***

[a] 3σ standard deviations are indicated in parenthesis. I = 0.15 M NaCl, T = 25 °C,

[b] pMn = −log[$Mn(II)_{free}$], $c_{Mn(II)} = c_L$ = 0.01 mM, pH = 7.4

For the better comparison of the ligands’ basicity, the sum of the protonation constants of the macrocycles have been calculated (logK_1 + logK_2 = ΣlogK_2) as well. Comparing *Σ*logK_2 values, one can conclude that the basicity of the $OPMMA^{2-}$ falls between those of the reference chelators. Based on the basicity of the $OPMMA^{2-}$, the logK_{MnL} of [Mn(OPMMA)] was expected to be higher than that of [Mn(OPC2A)]. Interestingly, the stability of the complex is 3 and 7 orders

of magnitude lower than that of [Mn(OPC2A)] and [Mn(3,9-PC2A)], respectively, due to the presence of the unsubstituted amine in the macrocyclic ring. The comparison of the pMns shows that the stability of our complex is more than two orders of magnitude lower than that of the comparative complexes.

III.6. Inertness of [Mn(OPMMA)]

The inertness of the [Mn(OPMMA)] complex was investigated by spectrophotometric method using Cu^{2+} ion as a scavenger for the OPMMA ligand in 10-fold excess to ensure the pseudo-first order conditions. The preliminary experiments showed that the dissociation of the [Mn(OPMMA)] is too fast to be investigated by conventional spectrophotometry, therefore stopped-flow method was used.

The k_{obs} values calculated from the absorbance-time data pairs increase with increasing $[H^+]$ showing a saturation-like behavior at higher pH values, indicating the formation of a relatively stable monoprotonated intermediate. The rate constant and the protonation constant (characterizing the proton-assisted dissociation pathway) obtained are presented in Table 6, where the corresponding values determined for the Mn^{2+} complex of $OPC2A^{2-}$ and 3,9-$PC2A^{2-}$ are also shown.

Interestingly, the $\log K_1^H$ value ($\log K_1^H = 4.67$) characterizing the protonation of the [Mn(OPMMA)] complex in the dissociation process was found to be one order of magnitude higher than that was determined for the [Mn(3,9-PC2A)] complex ($\log K_1^H = 3.55$). Furthermore, this protonation constant is also higher than those were determined for the carboxylates of the $OPMMA^{2-}$ ligand ($\log K_3 = 3.26$ and $\log K_4 = 1.29$). This phenomenon indicates that the protonation of the complex probably occurs directly on the unsubstituted macrocycle N donor, which seems to promote the faster release of the Mn(II) ion. In order to get a better comparison for the inertness of the three chelates, the half-lives ($t_{1/2}$) of the dissociation reactions have been also calculated for pH = 7.4 (Table 6).

Table 6. Rate and equilibrium constants for the dissociation of Mn^{2+} complexes of $OPMMA^{2-}$, $OPC2A^{2-}$ and 3,9-$PC2A^{2-}$ (I = 0.15 M NaCl, T = 25 °C, charges are omitted for simplicity).

Mn^{2+} complexes	OPMMA	OPC2A[b]	3,9-PC2A[c]
k_0 (s^{-1})	–	$(8.6\pm1.1)\times10^{-6}$	–
k_1 ($M^{-1}s^{-1}$)	$(1.4\pm0.1)\times10^{5}$	2.81±0.07	221±5
K_1^H	$(4.7\pm0.6)\times10^{4}$	–	$(3.6\pm0.5)\times10^{3}$
$t_{1/2}$(h)[a]	***3.5×10^{-2}***	***21.9***	***21.9***

[a] pH = 7.4

The $t_{1/2}$ values show that the inertness of [Mn(OPMMA)] is more than two orders of magnitude lower than that of the Mn^{2+} complexes of $OPC2A^{2-}$ and 3,9-$PC2A^{2-}$, probably because of the aforementioned reasons. The low inertness of the [Mn(OPMMA)] means that this chelate is not suitable for *in vivo* applications.

III.7. Relaxation features of [Mn(OPMMA)]

The longitudinal (r_{1p}) and transverse (r_{2p}) relaxation rates of the Mn^{2+} complex formed with $OPMMA^{2-}$ ligand have been determined (Table 7).

The relaxivity values of [Mn(OPMMA)] are slightly higher (except the r_{2p} relaxivities recorded at 60 MHz) than those of [Mn(OPC2A)] and [Mn(3,9-PC2A)]. The increased relaxivity can be the result of the asymmetric structure of the ligand, which results a more open structure.

Table 7. r_{1p} values ($mM^{-1}s^{-1}$) determined for Mn^{2+} complexes of $OPMMA^{2-}$ and other ligands used for comparative purposes at pH=7.4, 25/37 °C and 20/60 MHz (charges are omitted for simplicity).

	25/37 °C	OPMMA	OPC2A	3,9-PC2A
0.47 T	r_{1p}	3.48/2.84	3.13/2.54	2.91
	r_{2p}	5.85/4.70	5.15/4.17	3.96
1.41 T	r_{1p}	2.91/2.19	2.72/2.06	2.29
	r_{2p}	8.06/5.27	9.90/7.37	4.82

Since, the r_{1p} values of [Mn(OPMMA)] decrease with increasing temperature its relaxivity is controlled by fast rotation.

Based on the result gained from the NMRD and ^{17}O NMR measurements (Table 8), one can conclude that the water exchange rate of the [Mn(OPMMA)] is circa two-times higher than that was obtained for the [Mn(3,9-PC2A)] complex, and more than fourfold higher the that of [Mn(OPC2A)]. This behaviour surely the effect of the structural differences. The incorporation of the O atom into the macrocyclic structure can increase the rigidity of the coordination cage, in contrast, the asymmetric structure of the ligand decreases that. The small negative value of $\Delta S^{\ddagger}$ (-8 ± 1 $JK^{-1}mol^{-1}$) gained for the complex indicating associatively activated interchange mechanism for water exchange. The τ_{rH}^{298} is somewhat higher than that was obtained for [Mn(OPC2A)], which can be the result of the less compact structure of [Mn(OPMMA)].

Table 8. Best-fit parameters gained for [Mn(OPMMA)] from the analysis of ^{1}H NMRD and ^{17}O NMR data along with the corresponding values found for the Mn^{2+} complexes formed with $OPC2A^{2-}$ and 3,9-$PC2A^{2-}$ ligands (charges are omitted for simplicity).

Parameter	OPMMA	OPC2A	3,9-PC2A
k_{ex}^{298} ($\times 10^7$ s^{-1})[a]	22.1 ± 0.01	5.3	12.6
$\Delta H^{\ddagger}$ (kJ mol^{-1})[a]	23.1 ± 0.1	28.5	37.5
$\Delta S^{\ddagger}$ ($JK^{-1}mol^{-1}$)[a]	-8 ± 1	-1.9	–
E_{rH} / (kJ mol^{-1})[b]	17.2 ± 1.6	14.8	–
τ_{rH}^{298} (ps)[b]	55 ± 3	40.0	–
τ_{v}^{298} (ps)[b]	33 ± 11	19.3	–
Δ^2 ($\times 10^{19}$ s^{-2})[b]	2.1 ± 0.9	1.8	–

III.4. Calculated structure of [Mn(OPMMA)]

The DFT calculations delivered a capped trigonal prismatic coordination geometry for [Mn(OPMMA)] (Figure 3), in which all the donor atoms of the ligand are coordinated to the Mn(II) ion. The remaining coordination site is occupied by a water molecule which forms a strong hydrogen bond network with

the two second-sphere water molecules and one of the carboxylate pendant arms. The Mn(II)-O_{water} distance was calculated to be 2.35 Å which falls into the range of the first coordination shell of water. The $A_0/\hbar$ was estimated to be -39.8 $\times 10^6$ rad s^{-1} (A = –6.34 MHz) which is in the typical range for Mn(II) chelates and confirms the proposed structure in solution.

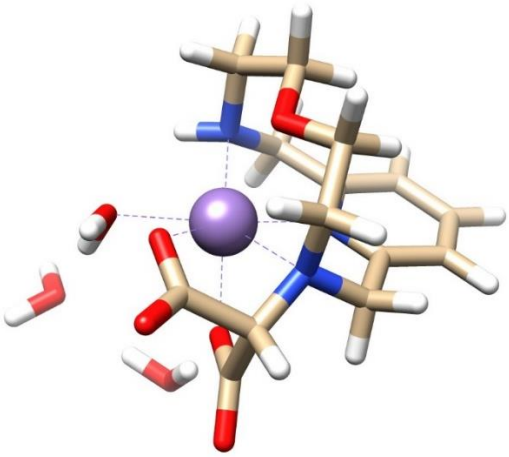

Figure 3. DFT optimized structure of the [Mn(OPMMA)] complex.

IV. Possible applications of the results

My PhD thesis is a fundamental research work connected to different fields of coordination chemistry.

Based on the obtained results, it is clear that the [Mn(OPMMA)] complex in its current form is not suitable for *in vivo* use, as its inertness falls far short of what is required for human applications. However, the synthesis of a derivative of the H_2OPMMA ligand has already begun, in which a *p*-methylbenzoic acid group is introduced onto the previously unsubstituted nitrogen. This modification is expected to significantly reduce the basicity of that nitrogen donor atom, thereby the resulting Mn(II) complex becomes more inert. This modification also opens the possibility of conjugating the ligand with peptides, making the resulting complex organ- or tissue-specific. Furthermore, with the use of a radioactive isotope such as ^{52}Mn, the complex could also become suitable for use in PET imaging studies.

In the case of the $[Gd(OPDMA)]^-$ complex, it can be said that although its properties surpass certain features of the open-chain Gd(III)-based MRI contrast agents currently in daily use, in its present form it is highly unlikely that the chelate we have developed will ever be used in practice, since the $[Gd(DOTA)]^-$ complex is still the best among contrast agents. The reason for this is that introducing a new contrast agent to the market requires an enormous investment of time and money. However, knowing that in the $[Gd(OPDMA)]^-$ complex one of the carboxylate groups of a malonate moiety does not coordinate to the metal ion, conjugation of the complex could also be feasible in this case. This modification opens new possibilities for its practical application, whether in diagnostics or in radiotherapy.

List of publications

Foreign language scientific articles in international journals:

1. **Exploring a rigid macrocyclic ligand bearing malonate pendants for Gd(III) complexation: the coordination chemistry of [Gd(OPDMA)]$^{-}$**

Abraham Estifanos Debretsion, Szilvia Bunda, Norbert Lihi, Gábor Papp, Agnés Pallier, Éva Jakab-Tóth and Ferenc Krisztián Kálmán

Inorganic Chemistry, **2025**, *64*(21), 10594-10602.

DOI: http://dx.doi.org/10.1021/acs.inorgchem.5c01224

2. **Stability and relaxometric characterization of a manganase(II) based macrocyclic complex containing malonate pendant**

Abraham Estifanos Debretsion, Szilvia Bunda, Norbert Lihi, Zoltán Garda, Emese Kun, Tibor Csupász, Gyula Tircsó, Éva Jakab-Tóth and Ferenc Krisztián Kálmán

Dalton Transactions, **2025**,

DOI: http://dx.doi.org/10.1039/D5DT01056J

Oral presentations:

1. **Bicyclic ligand family for Cu(II) chelation in radiodiagnostics**

Szilvia Bunda, Norbert Lihi, Ibolya Kálmán-Szabó, Zsófia Szaniszló, Tibor Csupász, Dezső Szikra, Abraham E. Debretsion, Gyula Tircsó, Judit Szabó Péliné, Anikó Fekete, Barbara Gyuricza, Dániel Szücs, Gábor Papp, György Trencsényi and Ferenc K. Kálmán

ISABC 16th, June 11-14, 2023, Ioannina Greece

2. **Synthesis of O-pyclen-based ligand containing malonate pendant for Mn(II) complexation and characterization of its Mn(II) chelate**

Abraham Estifanos Debretsion, Szilvia Bunda, Norbert Lihi, Zoltán Garda, Dóra Bakos, Emese Kun, Tibor Csupász, Gyula Tircsó, Éva Jakab-Tóth and Ferenc Krisztián Kálmán

57th Coordination Chemistry Conference, May 27-29, 2024, Szeged, Hungary

3. **Physico-chemical characterization of O-pyclen based Gd(III) and Mn(II) complexes, bearing malonate pendants**

Abraham Estifanos Debretsion, Szilvia Bunda, Norbert Lihi, Zoltán Garda, Agnés Pallier, Éva Tóth, Emese Kun, Tibor Csupász, Gyula Tircsó, Gábor Papp and Ferenc Krisztián Kálmán

58th Coordination Chemistry Conference, May 26-28, 2025, Balatonszárszó, Hungary

Posters:

1. **Investigation of OPMMA Ligand as MRI Contrast Agent**

Abraham Estifanos Debretsion, Szilvia Bunda, Norbert Lihi, ZoltánGarda, DóraBakos, EmeseKun, Tibor Csupász, Gyula Tircsó, Éva Jakab-Tóth and Ferenc Krisztián Kálmán

”The Future of Molecular MR” International Conference, June 17-20, 2024, Orléans, France

2. **Exploring rigid macrocyclic ligand bearing malonate pendants for Gd(III) complexation: the coordination chemistry of [Gd(OPDMA)]$^{-}$**

Abraham Estifanos Debretsion, Szilvia Bunda, Norbert Lihi, Agnés Pallier, Éva Jakab-Tóth and Ferenc Krisztián Kálmán

ISABC 17th, June 15-18, 2025, Uppsala, Sweden

UNIVERSITY AND NATIONAL LIBRARY
UNIVERSITY OF DEBRECEN
H-4002 Egyetem tér 1, Debrecen
Phone: +3652/410-443, email: publikaciok@lib.unideb.hu

Registry number: DEENK/425/2025.PL
Subject: PhD Publication List

Candidate: Abraham Estifanos Debretsion
Doctoral School: Doctoral School of Chemistry
MTMT ID: 10100793

List of publications related to the dissertation

Foreign language scientific articles in international journals (2)

1. **Debretsion, A. E.**, Bunda, S., Lihi, N., Papp, G., Pallier, A., Tóth, É., Kálmán, F. K.: Exploring a Rigid Macrocyclic Ligand Bearing Malonate Pendants for Gd(III) Complexation: the Coordination Chemistry of [Gd(OPDMA)].
   Inorg. Chem. 64 (21), 10594-10602, 2025. ISSN: 0020-1669.
   DOI: http://dx.doi.org/10.1021/acs.inorgchem.5c01224
   IF: 4.7 (2024)
2. **Debretsion, A. E.**, Bunda, S., Lihi, N., Garda, Z., Van Doorslaer, S., Kun, E., Csupász, T., Tircsó, G., Tóth, É. J., Kálmán, F. K.: Stability and relaxometric characterization of a manganase(II) based macrocyclic complex containing malonate pendant.
   Dalton Trans. Epub ahead of print, [1-22], 2025. ISSN: 1477-9226.
   DOI: http://dx.doi.org/10.1039/D5DT01056J
   IF: 3.3 (2024)

Total IF of journals (all publications): 8
Total IF of journals (publications related to the dissertation): 8

The Candidate's publication data submitted to the Tudóstér have been validated by DEENK on the basis of the Journal Citation Report (Impact Factor) database.

25 June, 2025

DEBRECENI EGYETEM Egyetemi és Nemzeti Könyvtár